C. R. Physique 17 (2016) 242–263

Contents lists available at ScienceDirect

Comptes Rendus Physique

www.sciencedirect.com

Condensed matter physics in the 21st century: The legacy of Jacques Friedel

Dislocations and other topological oddities

Dislocations et autres bizzareries topologiques

Pawel Pieranski

Laboratoire de physique des solides, Université Paris-Sud, bâtiment 510, 91405 Orsay cedex, France

ARTICLE INFO

Article history:
Available online 18 December 2015

Keywords:
Dislocations
Topological defects
Liquid crystals

Mots-clés :
Dislocations
Défauts topologiques
Cristaux liquides

ABSTRACT

We will show that the book *Dislocations* by Jacques Friedel, published half a century ago, can still be recommended, in agreement with the author's intention, as a textbook "*for research students at University and for students at engineering schools as well as for research engineers*". Indeed, today dislocations are known to occur not only in solid crystals but also in many other systems discovered more recently such as colloidal crystals or liquid crystals having periodic structures. Moreover, the concept of dislocations is an excellent starting point for lectures on topological defects occurring in systems equipped with order parameters resulting from broken symmetries: disclinations in nematic or hexatic liquid crystals, dispirations in chiral smectics or disorientations in lyotropic liquid crystals. The discussion of dislocations in Blue Phases will give us an opportunity to call on mind Sir Charles Frank, friend of Jacques Friedel since his Bristol years, who called these ephemeral mesophases "topological oddities". Being made of networks of disclinations, Blue Phases are similar to Twist Grain Boundary (TGB) smectic phases, which are made of networks of screw dislocations and whose existence was predicted by de Gennes in 1972 on the basis of the analogy between smectics and superconductors. We will stress that the book by Jacques Friedel contains seeds of this analogy.

RÉSUMÉ

Nous allons montrer que l'ouvrage *Dislocations* de Jacques Friedel, publié voici un demi-siècle, peut toujours être recommandé, ainsi que le voulait l'auteur, comme un manuel « *pour des étudiants chercheurs universitaires et pour des élèves d'écoles d'ingénieurs, aussi bien que pour des ingénieurs chercheurs* ». En effet, les dislocations sont connues aujourd'hui pour intervenir non seulement dans les cristaux solides, mais aussi dans de nombreux autres systèmes découverts plus récemment, tels que les cristaux colloïdaux ou des cristaux liquides avec des structures périodiques. De plus, le concept de dislocation constitue un excellent point de départ des exposés sur les défauts topologiques dans les systèmes munis de paramètres d'ordre résultant de symétries brisées : disinclinaisons dans des cristaux liquides nématiques ou hexatiques, dispirations dans les phases smectiques chirales ou disorientations dans les cristaux liquides lyotropes. La discussion sur les dislocations dans les phases bleues nous fournira une occasion pour nous souvenir de Sir Charles Frank, un ami de Jacques Friedel depuis ses années à Bristol, qui appelait ces mésophases éphémères « bizarreries topologiques ». Étant formées de réseaux de disclinations, les

E-mail address: pawel.pieranski@u-psud.fr.

http://dx.doi.org/10.1016/j.crhy.2015.12.002

phases bleues sont similaires aux phases smectiques à joints de grains torsadés (*Twist Grain Boundaries*, TGB), qui sont constituées de réseaux de dislocations vis et dont l'existence a été prévue par de Gennes en 1972 à partir de l'analogie entre les phases smectiques et les supraconducteurs. Nous insisterons sur le fait que le livre de Jacques Friedel contient les germes de cette analogie.

1. Introduction

1.1. The Bristol chock

In chapters "Le choc de Bristol (1949–1952)" and "Le pied à l'étrier" of his memories "*Graine de mandarin*" [1], Jacques Friedel tells in what circumstances he "got a foot on the ladder" of his exceptionally long and glorious career as a university teacher, fully involved in fundamental research. He emphasizes on the importance of his three-year-long stay in Bristol (1949–1952) where, in the week following his arrival, he attended a scene that became famous in the history of the solid-state physics: "*(Presumably during a seminar) Charles Frank was describing results of calculations, made with W.K. Burton and N. Cabrera [2], of spiral-like shapes of steps connected to dislocations emerging on a facet of a growing crystal when somebody in the audience got up and showed spirals of identical shapes he observed on quartz surfaces* (see Fig. 1).". This incident, which impressed a lot the young French visitor and triggered his interest in dislocations, was usual in Bristol where talented researchers were exploring new areas with enthusiasm and confidence.

It is interesting to emphasize that the interest of Frank him-self in crystal growth was accidental too. We know that from his Crystal Growth Award Address whose written version was published in Ref. [3]:

"I came into the subject of Crystal Growth partly by what I may call a geographic accident, namely that I had a room at the Bristol Laboratory adjacent to that of Keith Burton, who was being payed by I.C.I. explicitly to do research under Mott on the theory of crystal growth (this was one of the rather rare examples of a targeted research in fundamental science which made some progress toward its designated target). [...] Mott [...] asked me to give three or four seminars on nucleation theory. In my fourth seminar I presented Volmer's theory of the rate of crystal growth [...]. Keith Burton was in a position to make some reasonably reliable estimates so as to put numbers in Volmer's algebra. And when that was done we found that at 1 percent supersaturation the experimental growth rate was about 10^{1000} times larger than the theory said: we remarked that that was the largest factor of discrepancy we had ever seen called agreement. Oddly, I needed the shock of that big number to make me take seriously an idea which I had previously produced only as a mental squib – namely that we knew crystals were full of dislocations (not always! see [4]) *– that a dislocated crystal was not a stack of layers but one layer complicatedly overlapping itself, so it need never start a new layer."*

1.2. 1964: the textbook on dislocations

After his return to France, Jacques Friedel had contacts with several research teams in the Paris area and realized that all he learned in Bristol about dislocations interested many people, so he started to give lectures on this subject first in the "École de mines" (Paris), then at IRSID (Steel Research Institute, Saint-Germain-en-Laye). These lectures resulted in the textbook *Dislocations* [5], whose first French version was published in 1956. One can read in *Graine de mandarin* [1] that "*I wrote successive chapters in the train on the way from the Saint-Lazare Station to Saint-Germain. I included all I learned, in particular with C. Crussard and F.C. Frank. I also added a number of my personal contributions, concerning principally dislocation networks, their stability and evolution upon thermal or mechanical processing. I also discussed the role, played in plasticity, by the core of dislocations as well as by the crystalline structure and the nature of interatomic interactions. The first edition of 1000 copies was sold in a few months; three wild American versions appeared too, which I took as a compliment in the domain opened recently by books of A. Cottrel and W.T. Read.*".

1.3. Fifty years later: dislocations in soft condensed matter

Even if, as stated in the Preface of the Jacques Friedel's *Dislocations*, "*it has been written essentially for metallurgists*", most of its content applies to all kinds of crystals, not only for metals. Indeed, in his book Jacques Friedel deals mostly with general concepts whose validity is independent of structural details such as the chemical nature of atoms or molecules. For this reason, the book is illustrated by images of defects not only in metals but also in non-metallic materials such as SiC, LiF, MgO, KCl, Ge, Si, AgCl, CaF_2.

Fifty years later, beside these solid three-dimensional crystals, dislocations are known to occur in other systems such as colloidal crystals or thermotropic and lyotropic mesophases equipped with a translational or orientational periodic order. Our aim here is to review shortly these new domains of application of general concepts treated by Jacques Friedel in his book. To start with, we will focus on dislocations occurring in colloidal crystals. As we will see in section 2.2, when working on this topic, we benefited not only from reading Jacques Friedel's book, but also from his kind personal help.

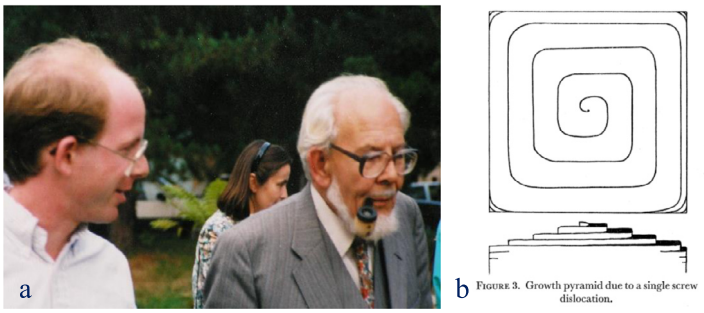

Fig. 1. Charles Frank, friend of Jacques Friedel since Bristol years: a) smoking a pipe and walking with John Bechhoefer during the Jacques Friedel's Jubilée in Orsay, b) figure from the generic paper of Burton, Cabrera and Frank [2].

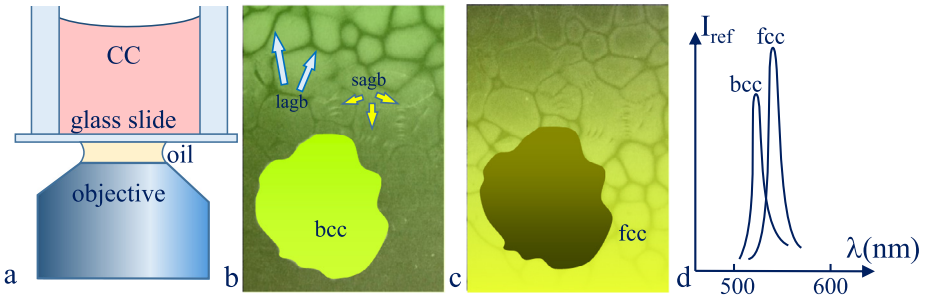

Fig. 2. Coexistence of fcc and bcc crystallites detected by means of the microspectrometry: a) setup, b) $\lambda_{110} = 527$ nm, bright Bragg reflection from the bcc crystallite in the center, c) $\lambda_{111} = 542$ nm, bright Bragg reflection from fcc crystallites surrounding the bcc crystallites, d) spectra of Bragg reflections. Blue and yellow arrows in b point respectively to large-angle grain boundaries (lagb) and small-angle grain boundaries made of dislocations (sagb).

2. Colloidal crystals

2.1. Polycrystalline texture

The term "colloidal crystals", coined by Shaefer, Ackerson and Clark [6,7] (see also Refs. [8,9]) designates suspensions of colloidal particles ordered into two- or three-dimensional lattices. In the case of polystyrene spheres ≈ 0.1 μm in diameter dispersed in water, fcc or bcc structures can occur. In special conditions of concentration and ionic purity, fcc/bcc phase coexistence has been observed by means of a reflecting microscope in monochromatic illumination, as shown in Fig. 2 [10].

The texture of the colloidal crystal sample shown in Fig. 2b and c is polycrystalline. Crystallites are oriented with their most dense crystal planes parallel to the glass slide: (110) for bcc and (111) for fcc. Crystallites are separated by grain boundaries. Large-angle grain boundaries (lagb) pointed by blue arrows appear as black lines because CC is melted there. Small-angle grain boundaries (sagb) made of dislocations are pointed by yellow arrows in Fig. 2b.

2.2. Generation of dislocations by confinement

With the aim to generate dislocations in a well-controlled way, the sample of a colloidal crystal has been confined between a glass slide and a glass sphere as shown in Fig. 3a (for details, see Ref. [11]). In the image in Fig. 3b, we identify edge dislocations as lines across which the color of the reflected light varies sharply. The internal side of each dislocation line is reddish, while the color on its external side is shifted to green. The experimental setup was equipped with a system allowing one to control the gap h_o between the glass sphere and the slide with an accuracy of 0.01 μm. When the gap is reduced, new dislocation loops are generated in the center of the target-like pattern.

We had an opportunity to present these observations to Jacques Friedel, who found them interesting and calculated the energy of dislocations confined between two walls making an angle α. The manuscript of this calculation (see Fig. 4b), starts with the drawing representing the system of real dislocations located in the wedge-shaped crystal and surrounded by a set of mirror dislocations whose presence is imposed by boundary conditions: the perfect rigidity of the wedge walls. The accompanying text reads: "*On a une collection de dislocations coin. Les conditions aux limites rigides sont équivalentes à l'adjonction de dislocations images.*".

Labels $n-1$ and n refer to the number of crystal planes confined in the wedge respectively on the left and right sides of the dislocation. The radius of the dislocation core is labeled as r_o. Let x_d be the x coordinate of the dislocation. Then $h = \alpha x$ is the local thickness of the wedge. In the first approximation, one can say that if p_o is the equilibrium thickness of crystal layers then at $x_{n-1} = (n-1)p_o/\alpha$ and $x_n = np_o/\alpha$ the crystal is not deformed. For $x_{n-1} < x < x_d$, the crystal is stretched

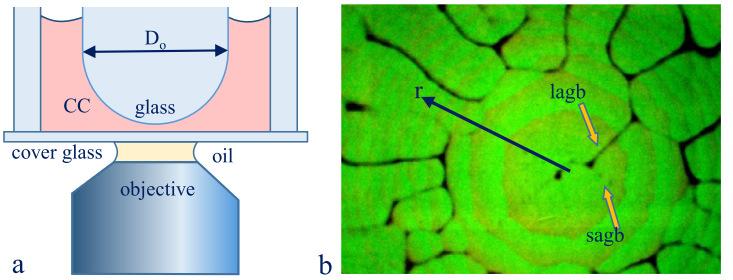

Fig. 3. System of edge dislocation in a colloidal crystal confined between a glass sphere and a glass cover slide: a) scheme of the setup, b) image taken with an inverted reflecting microscope equipped with an immersion objective. Variations of colors unveil strains in the vicinity of dislocations. Arrows point large angle grain boundaries (lagb) which are melted and small angle grain boundaries (sagb) made of dislocations visible as black dots.

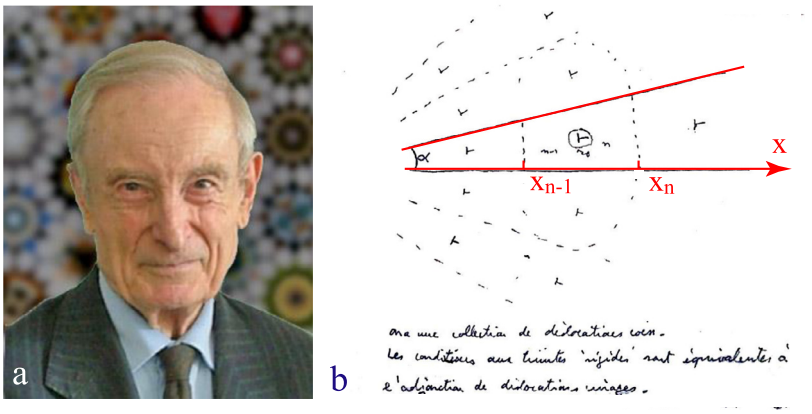

Fig. 4. Jacques Friedel (a) and the beginning of his hand-written calculation of the energy of a system of dislocations (b). One can read: *On a une collection de dislocations coin. Les conditions aux limites rigides sont équivalentes à l'adjonction de dislocations mirages.* (Annotations in red have been added with the aim to improve the readability of a pencil-made drawing.)

while for $x_d < x < x_n$ it is compressed. Therefore the elastic energy per unit length stored in the band between x_{n-1} and x_n can be written approximatively as:

$$W_{/m} \approx \frac{1}{2}E\left(\int_{o}^{\xi_d}\frac{(\alpha\xi)^2}{(n-1)p_o}d\xi + \int_{\xi_d}^{p_o/\alpha}\frac{(p_o-\alpha\xi)^2}{np_o}d\xi\right) \tag{1}$$

where E is the Young modulus in the isotropic approximation and $\xi = x - x_{n-1}$. For large values of n, one obtains then:

$$W_{/m} \approx \frac{1}{2}\frac{E\alpha}{n}\left[\xi_d^2 - (p_o/\alpha)\xi_d + \frac{1}{3}(p_o/\alpha)^2\right] \tag{2}$$

It is not surprising that this elastic energy is minimal when the dislocation is located at $\xi_d = p_o/(2\alpha)$ that is to say in the middle between x_{n-1} and x_n where

$$h = \left(n - \frac{1}{2}\right)p_o \tag{3}$$

From formula (2), one calculates the force acting on the dislocation as a function of its position in the wedge.

$$F_{/m} = \frac{dW}{d\xi_d} = \frac{E\alpha}{n}[\xi_d - p_o/(2\alpha)] \tag{4}$$

In our experiment, the "spring constant" $E\alpha/n$ of this elastic force varies with the distance r from the center of the gap because (1) the slope α grows with r, and (2) the number of crystal planes grows with r too. As a result,

$$\frac{E\alpha}{n} \approx 2Ep_o\frac{r/D_o}{h_o + r^2/D_o} \tag{5}$$

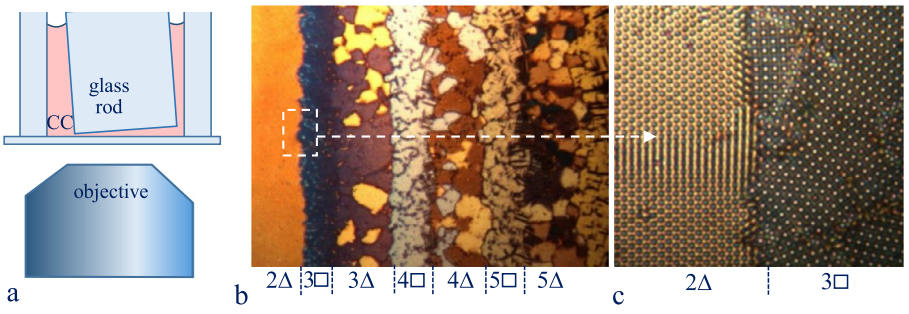

Fig. 5. Series of structures in a suspension of hard spheres confined in a wedge formed by two glass walls: a) geometry of the setup, b) view in transmitted light at low magnification, c) view of the $2\Delta \Rightarrow 3\square$ frontier at high magnification. (PhD work of B. Pansu.)

This function has a maximum at $r_{\max} = \sqrt{h_o D_o}$. In the experiment, this "spring constant" determines the amplitude of deviations from the circular shape of dislocations. For this reason, dislocation loops are the most irregular in the center (see Fig. 3b).

2.3. Unexpected structural transitions

The colloidal crystal used in the experiment discussed above was made of polystyrene spheres, about 0.1 μm in diameter, dispersed in water. When the Bragg reflection (from (111) planes of the fcc crystal) is green, with the wavelength $\lambda = 0.534$ μm, the mean distance a_s between the centers of the particles can be estimated as 0.23 μm, *i.e.* twice their diameter. In this case, the crystalline order (fcc or bcc) results from the electrostatic repulsion between the polystyrene spheres, which are negatively charged on their surfaces. Screened by counterions and other ionic impurities, the range of this interaction is finite, still longer than the interparticle distance. As a result, this kind of colloidal crystal is elastically soft and can support strains, resulting from the confinement, without structural transitions.

Experiments with colloidal crystals made of large polystyrene spheres, about 1 μm in diameter, unveil a very different and quite complex behavior.

The experimental setup depicted in Fig. 5a is almost identical to the one in Fig. 3a, except for three details: (1) the glass sphere is replaced by a glass cylinder whose bottom and top surfaces are polished, (2) the cylinder's tilt and its distance from the glass slide are controlled precisely, (3) the transmitted illumination is used instead of the reflecting one. In this setup, the colloidal suspension is confined between two glass walls forming a wedge.

Images in Figs. 5b and c show a series of structures occurring as a function of the gap thickness. The first yellow band on the left-hand side of Fig. 5b corresponds to a stack of two layers in which the 2D order is triangular. The next blue band is a stack of three layers in which the 2D order is square. The following band has a "patchy" bi-colored aspect and is a stack of three "triangular" layers. In summary, confinement of 1 μm polystyrene spheres in a wedge leads to the following sequence of structures:

$$2\Delta \Rightarrow 3\square \Rightarrow 3\Delta \Rightarrow 4\square \Rightarrow 4\Delta \Rightarrow 5\square \Rightarrow \cdots n\square \Rightarrow n\Delta \tag{6}$$

In Fig. 5, all stacks of layers with the square order appear as bands of uniform color, while stacks of triangular layers are "patchy" when $n > 2$. The number of different colors $N_c(n)$ in stacks of n triangular layers grows with n: $N_c(2) = 1$, $N_c(3) = 2$, $N_c(4) = 3 \ldots$.

Obviously, $N_c(n)$ is related to the number of different stacks that can be realized with n layers. The book of Jacques Friedel is helpful in this matter. In section 6.2.2, "Face centered cubic metals and other structures", he reminds of the system introduced by Nabarro and Frank: instead of labeling layers with three letters, a, b and c, successive pairs of adjacent layers are labeled with two symbols, Δ and ∇. This convention is explained in Fig. 6a. Let us consider an **arbitrary** layer of the stack. In Fig. 6a, it is represented as the layer of close-packed spheres labeled "a". The next layer can be located either in sites represented by the triangle Δ or in sites represented by the inverted triangle ∇. In this convention, the stack of n layers is represented by a sequence of $n-1$ Δ-s or ∇-s. The fcc structure corresponds to sequences $\Delta\Delta\Delta\Delta\ldots$ or $\nabla\nabla\nabla\nabla\nabla\ldots$, while the hcp structure is represented by the alternating sequence $\nabla\Delta\nabla\Delta\nabla\Delta\ldots$. Optically, two stacks are equivalent if they are related by a rotation around a two-fold axis passing through the center of any sphere and orthogonal to the layer. Upon this symmetry operation, ∇ is replaced by Δ and *vice versa*. Using this property, the four possible sequences of three layers are arranged into two pairs bb' and cc' where b ($\nabla\nabla$) is equivalent to b'($\Delta\Delta$) and c ($\nabla\Delta$) is equivalent to c' ($\Delta\nabla$). In stacks of four layers, three pairs of optically different sequences are possible. For the purpose of simplicity, only one member of each pair is represented in Figs. 6d, e and f.

Experiments reported in references [12] and [13] were made with relatively concentrated suspensions in which the polystyrene spheres of diameter $\Phi \approx 1$ μm were almost close-packed. Van Winkle and Murray [14] performed much more accurate experiments with samples in which the average distance between spheres $a_s = (1/n)^{1/3}$ ranged between 2Φ and 6Φ. Samples were confined between parallel plates and structures were detected both by direct observation and by light

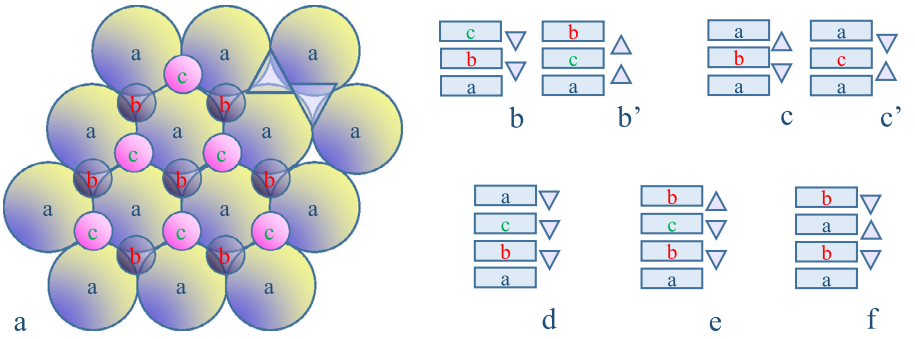

Fig. 6. Explanation of the "patchy" aspect of stacks of triangular layers: a) definition of a, b and c positions in stacks of triangular layers, b and b') two stacks of three optically equivalent layers, c and c') two other stacks of three optically equivalent layers, d, e and f) three stacks of four optically different layers.

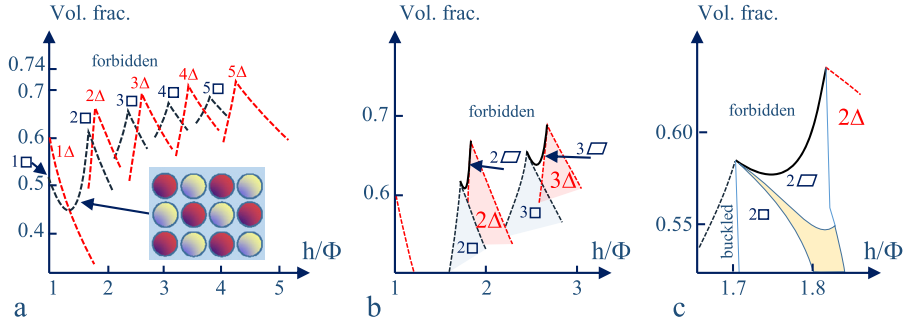

Fig. 7. Theory of structural transitions: a) high-pressure limit, stacks of triangular and square layers [15]; the inset shows alternating "up" and "down" motions splitting one square layer 1□ into the stack 2□ of two square layers, b) high-pressure limit, dashed lines: stacks of triangular and square layers [15]; plain lines: rhombic deformation of square stacks, c) result of the Monte Carlo simulation performed by Schmidt and Löwen [16]. (Domains labeled "forbidden" are not accessible without overlapping of particles.)

scattering. The remarkable result of this study is that the sequence of structures given in Eq. (6) occurs as a function of the relative thickness D/a_s.

The first explanation of the observed sequence of structures was given in the frame of a model of the best packing of hard spheres. In Fig. 7a [12], the volume fraction calculated for stacks of square and rectangular layers is plotted as a function of the reduced thickness h/Φ. Obviously, when the gap thickness h grows, the best packing fraction is obtained alternatively with stack of triangular and square layers, as observed in experiments.

A more detailed analysis has shown that a continuous transition between $n\square$ and $n\Delta$ structures is possible by shear deformation in the plane of the sample. If one starts from a $n\square$ structure, the shear deforms the 2D square order in layers into a rhombohedric lattice. When the acute angle of rhombs reaches the value of $\pi/3$, one obtains an *ababab*... stack of triangular layers corresponding the hcp structure. As shown in Fig. 7b, during this transition the volume fraction evolves on black lines connecting adjacent $n\square$ and $n\Delta$ summits.

2.4. $1\Delta \Rightarrow 2\square$ *transition, a topological oddity*

In the frame of the best-packing-hard-spheres model, it is much more difficult to find continuous transitions between structures with different numbers of layers. This difficulty is obvious if one considers the simplest case of the $1\Delta \Rightarrow 2\square$ transition. To start with, let us consider first a square monolayer $1\square$ that is easy to split into two square layers by "up" and "down" motions of nearest neighbors (see the inset in Fig. 7a). In this case, as shown in Fig. 7a, the volume fraction evolves on the line connecting the point $1\square$ with the summit $2\square$.

However, if one starts with a triangular monolayer (see Fig. 8a) and tries to divide it into two layers by "up" and "down" motions in **all pairs of** nearest neighbors (see Fig. 8b), it becomes obvious that this is an impossible task similar to the one encountered in the Ising antiferromagnetic model on a triangular lattice. In experiments, this frustration results in strong fluctuations of particles moving "up" and "down".

These frustration-induced fluctuations discovered in suspensions of polystyrene spheres (Fig. 3D in Ref. [13]) have been studied in details recently by Shokef et al. [17] in a very astute system especially well adapted for this purpose: an aqueous suspension of microgel spheres composed of cross-linked NIPA (*N*-isopropyl acrylamide) polymers. The crucial advantage of this system is that, in contradistinction with suspensions of polystyrene spheres, it allows a continuous *in situ* variation of the free volume fraction at constant particle density. Indeed, microgel spheres made of the NIPA cross-linked polymer

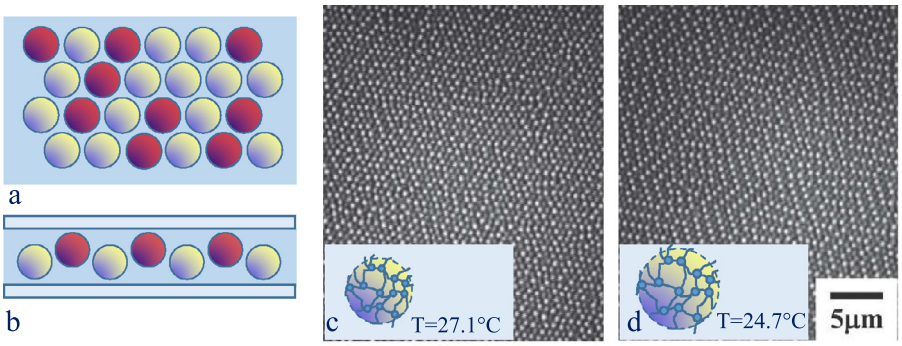

Fig. 8. Buckling transition in a monolayer of N-isopropyl acrylamide microgel spheres dispersed in water and confined between two glass plates: a–b) schematic representations of the sample, top and side views, c–d) optical images taken at $T = 27.1\,^{\circ}\mathrm{C}$ and $24.7\,^{\circ}\mathrm{C}$. (Adapted from reference [17] with permission of The Royal Society of Chemistry.)

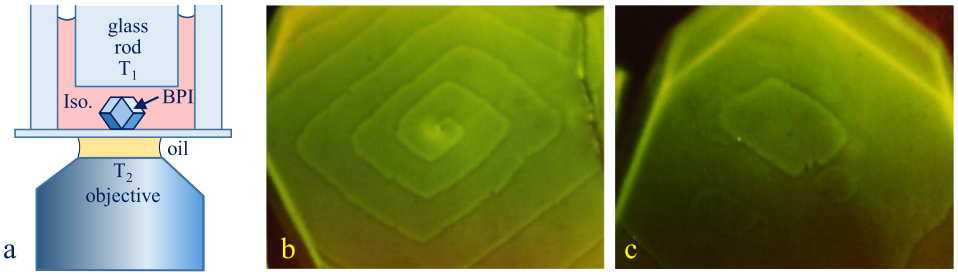

Fig. 9. Observation of the growth of a BPI crystal from the isotropic phase (Iso.): a) experimental set-up. Temperatures T_1 and T_2 are regulated with an accuracy of $0.01\,^{\circ}\mathrm{C}$, $T_2 < T_1$, b) growth of the BPI crystal by the spiral motion of the step connected to the dislocation emerging on the (110) facet at isotropic/BPI interface, c) growth of the BPI crystal by nucleation of steps on the (110) facet. Photographs taken with a reflecting microscope in monochromatic illumination with the wavelength $\lambda = 558$ nm tuned to the Bragg reflection from (110) crystal planes. Knowing that the average refractive index of BPI is $n \approx 1.5$, one obtains from the Bragg formula the interplanar distance $h_{110} = \lambda/(2n) = 186$ nm. Composition of the sample: 58.5% of CB15 in ZLI1140. (Collaboration with P.E. Cladis and R. Barbet-Massin.)

contain about 96% of water at $T = 20\,^{\circ}\mathrm{C}$ and their hydrodynamic diameter is 850 nm. Upon heating to $T = 30\,^{\circ}\mathrm{C}$, water is partially squeezed out from the microgel spheres so that their diameter decreases to 650 nm while the total volume of the system "microgel spheres + water" and the particle density are conserved.

One of remarkable results obtained by Shokef et al. concerns the dynamics of "up" and "down" fluctuations. Using image processing, the two-level $z_i(t) = \pm 1$ trajectory of individual particles was recorded and the two-time correlation function $C(t) = \langle z_i(0) z_i(t) \rangle$ function was found to decay as a stretched exponential of time

$$C(t) = \exp\left[-(t/\tau)^{\beta}\right] \tag{7}$$

Upon cooling from $T = 27.1\,^{\circ}\mathrm{C}$ to $24.7\,^{\circ}\mathrm{C}$, the relaxation time τ was found to increase by five orders of magnitude from 10^{-1} s to 10^{4} s with the stretching exponent decreasing from 0.8 to 0. This slowing-down dynamics of fluctuations is accompanied by in-plane distortions of the triangular lattice leading to the zigzagging stripes shown in Fig. 8d.

3. Faceted liquid crystals: Blue Phases

3.1. Crystal habit and crystal growth

The very first photograph (Fig. 1.11 untitled *Growth spiral on silicon carbide*) in Jacques Friedel's book shows *a spiral-like step connected to a dislocation emerging on a facet of a growing crystal* (quotation from Jacques Friedel's autobiography, see section 1.1). Then, in the introduction of the chapter VII, "Crystal growth", one reads: *"Observation of growth figures on crystal grown from the vapor phase or in solution provided one of the most direct proofs that real crystals nearly always contain dislocations."*.

In Fig. 9b, we see also a spiral-like step connected to a dislocation, but this photograph **does not show a growing solid crystal**. Here, we see the **growth of a monocrystal of a liquid crystalline phase**, called Blue Phase I (BPI), from the isotropic phase. This photograph was taken in a reflecting microscope in monochromatic (green) illumination whose wavelength $\lambda = 558$ nm was tuned to the Bragg reflection from (110) planes of a structure periodic in three dimensions. The wavelength of the reflected light being about 500 times longer than that of X-rays reflected from solid crystals, we can conclude already that unit cells composing this liquid crystalline structure contain about 10^8 more molecules than unit cells of solid crystals. As it would be very difficult to assign fixed (x, y, z) positions to such a crowd of molecules, they are free to move like in

the liquid isotropic phase, but their orientations (locally expressed by the unit vector $\vec{n}$ called director) are ordered. Before a more detailed discussion of the orientational pattern $\vec{n}(x, y, z)$, let us see what other conclusions can be drawn from the shape of BPI crystals.

The whole habit (determined from other photographs) of the Blue Phase I is symmetrical with respect to a system of two-fold, three-fold, and four-fold symmetry axes. Taken together, they form the point symmetry group $O(432)$ so that the Bravais lattice of BPI must be cubic. Moreover, all types of facets occurring on the crystal habit form the following series in the order of their prominence:

$$(110) > (211) > (310) > (222) > (321) > \ldots \tag{8}$$

Following the empirical rules of faceting (enounced in [18] and explained, *e.g.*, in Ref. [19]) established by George Friedel [20] (the grand-father of Jacques Friedel), J.D.H. Donnay and D. Harker, this sequence is the fingerprint of the $I4_132$ (or O_8) symmetry.

In Fig. 9 the BPI crystal is oriented with the (110) facet parallel to the glass slide. The step nucleated and growing on the (110) facet (see Fig. 9c) has a rhombic shape compatible with the 2-fold symmetry axis perpendicular to this facet. Knowing the wavelength $\lambda = 558$ nm of the reflected light and the (mean) refractive index $n \approx 1.5$, one calculates the size of the cubic unit cell $a = \sqrt{2}h_{110} = 263$ nm. As we have already said above, such a huge unit cell contains about 10^8 molecules forming a peculiar orientational pattern that we will describe below.

3.2. Structure of Blue Phases: topological oddities

"[Blue Phases] are totally useless, I think, except for one important intellectual use, that of providing tangible examples of ***topological oddities****, and so helping to bring topology into the public domain of science, from being the private preserve of a few abstract mathematicians and particle theorists."* This opinion is no more fully true today because Blue Phases are starting to find applications in displays (see, *e.g.*, in [21]). However, in 1983, when Sir Charles Frank pronounced it, the Blue Phases have been known to occur only in a very narrow temperature interval of a few tenths of °C squeezed between the isotropic and cholesteric phases. For this reason, in the experiment discussed above, the sample – the mixture of 58.5% of CB15 (chiral compound) with ZLI1140 (a commercial eutectic nematic mixture) – is held between two glass surfaces whose temperatures T_1 and T_2 are regulated with an accuracy of 0.01 °C. BPI crystals nucleate from the isotropic phase and grow on the glass slide because its temperature T_2 is slightly lower than the one of the glass cylinder above, T_1.

The narrowness of the temperature range of Blue Phases is related to the so-called chiral frustration: **the impossibility to satisfy globally the local tendency of chiral molecules to adopt twisted configurations** (for a review on Blue Phases, see, *e.g.*, Ref. [22]). As we have no place here for a more detailed discussion on this fascinating problem, let us just say that two adjacent chiral molecules, like the two screws shown in Fig. 10a, would like to adopt a twisted configuration. If one molecule is oriented along the z axis, then all adjacent molecules will be twisted with respect to it. If this axisymmetric construction is continued, one obtains a so-called double-twist cylinder. Unfortunately, when the distance r from the axis z grows, the requirement of the twisted configuration in the direction orthogonal to r is less and less satisfied, and the construction must be stopped when the tilt angle with respect to the z axis reaches 45°. Usually, such double-twist cylinders are then assembled into cubic structures having $I4_132$ or $P4_232$ symmetries.

Here, instead of this classical model of the Blue Phase I we use an alternative one, depicted in Figs. 10b, c and d, which is constructed using the periodic minimal surface of symmetry *Ia3d* called gyroid. The reason for such a choice is that in the next section 4 we will deal with dislocations in cubic lyotropic phases whose structure is based on periodic minimal surfaces too. Our construction of the Blue Phase I is based on the fundamental property of minimal surfaces. By definition, the surface is said to be minimal if its mean curvature is zero at every point. In Fig. 10b, the lines of principal curvatures C_1 and C_2 in the point P are crossing at right angle. The lines of zero curvature, called asymptotic lines, A_1 and A_2 are bisecting C_1 and C_2. They provide a parameterization of the surface. On minimal surfaces, the two systems of parametric lines taken separately can be seen as two director fields of opposite chirality. By choosing one of them (A_2 in Fig. 10b), the double-twist director field can be built as shown in Fig. 10b.

The whole director field of the Blue Phase I can then be assembled from one elementary piece, shown in Fig. 10c, using symmetry operations of the space group $I4_132$. Now, the director field constructed by this means contains necessarily singular lines called disclinations because the minimal surface G contains the so-called flat points F in which principal curvatures are zero. Indeed, when one examines the vicinity of the point F in Fig. 10c, it is obvious that the director field is singular here: the orientation of molecules at point P is undetermined. For experts in liquid crystals, it is obvious that the director field in the vicinity of the point P has the structure typical of a $-1/2$ disclination (in two dimensions). The red arrow passing through the point P is a three-fold symmetry axis. For symmetry reasons, the director field must be singular all along this axis, not only at point P. We have therefore to do with a singular line of the director field – a disclination line. All other three-fold axes of the $I4_13$ space group must also be singular. In conclusion, the Blue Phase I can be seen as a periodic network of disclination lines. This is the reason for which Charles Frank considered Blue Phases as *topological oddities*.

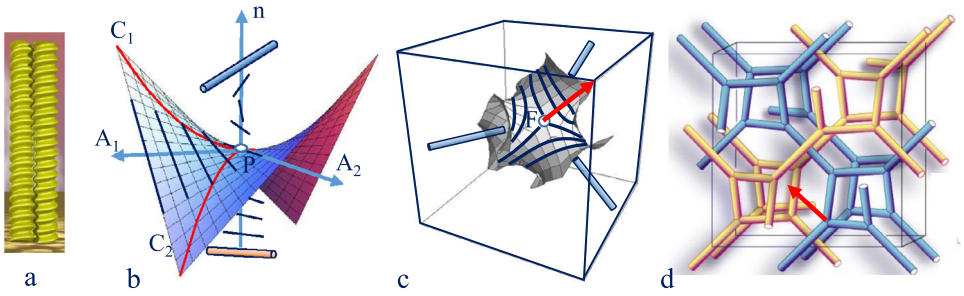

Fig. 10. Model of the BPI phase of symmetry $I4_132$ built around the periodic minimal surface G (gyroid) of symmetry $Ia3d$. a) Two adjacent chiral molecules, like two screws matching their threads, have the tendency to adopt a twisted configuration. b) Double-twist configuration around the molecule located in P. c) An elementary piece of the minimal surface G. The whole surface G can be built from such pieces. At F, the flat point, principal curvatures are zero. Thick lines represent a chiral director field **n** that has a singularity at F: a $-1/2$ disclination. d) two labyrinths separated by the surface G.

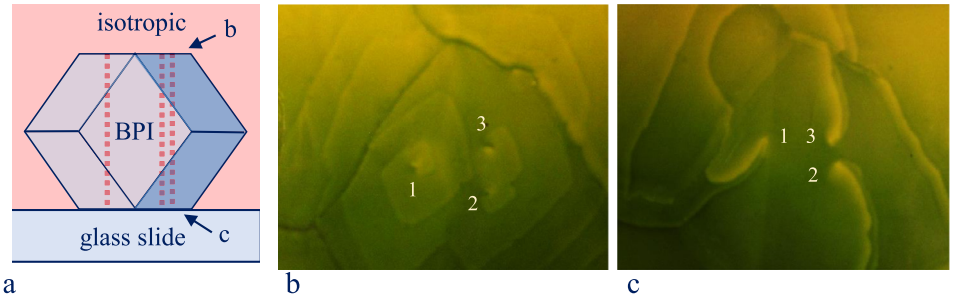

Fig. 11. Three dislocations piercing the BPI crystal. a) Side view of the setup, dislocations are drawn with dotted lines. b) Focus on the isotropic/BPI interface. c) Focus on the BPI/glass interface. Photographs taken with a reflecting microscope in monochromatic illumination. (Collaboration with P.E. Cladis and R. Barbet-Massin.)

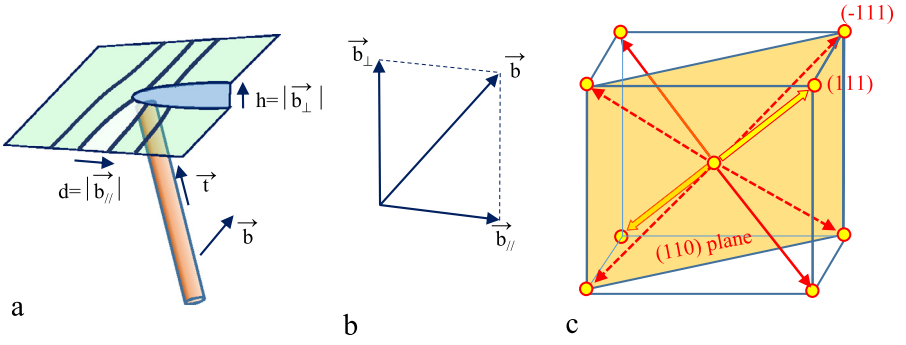

Fig. 12. Relationship between Burgers vectors and steps connected to dislocations. a) Dislocation emerging on a facet. The height h of the step connected to the dislocation depends on the length of the component perpendicular to the facet. b) Decomposition of the Burgers vector into components respectively parallel and perpendicular to the facet. c) Orientation of Burgers vectors with respect to the (110) facet.

3.3. Steps connected to dislocations and their motions

Knowing that the Bravais lattice of BPI is bcc, we can ask now what is the Burgers vector of the dislocation emerging on the (110) facet in Fig. 9b. The same question can be asked about three dislocations emerging at the BPI/isotropic interface where they give rise to steps as shown in Fig. 11b. Let us note that all three dislocations pierce the whole crystal (see Fig. 11a) and give rise to "double steps" at the BPI/glass interface too (see Fig. 11c).

In the search for the answer, let us remind shortly explanations given by Jacques Friedel in section 1.4.2. of his book. Let $\vec{b}$ be the Burgers vector of a dislocation emerging on a facet (see Fig. 12a) and $\vec{b}_{//}$ and $\vec{b}_{\perp}$ be components of $\vec{b}$ respectively parallel and perpendicular to the facet (Fig. 12b). The dislocation gives rise to a step of height $h = |\vec{b}_{\perp}|$. In the case of BPI crystals, eight (the shortest) Burgers vectors are possible. Four of them, drawn with dotted arrows in Fig. 12c, are parallel to the facet, so that their emergence on the (110) facet does not give rise to steps. The four other Burgers vectors make the same angle with the (110) plane, so that they should give rise to steps of the same height $h = a/\sqrt{2}$.

In Fig. 11, the BPI crystal is pierced by three dislocations connected to steps. (Remarkably, this configuration is almost identical to the one in Fig. 7.3 of Jacques Friedel's book.) Dislocations 2 and 3 are connected by the step, which means that

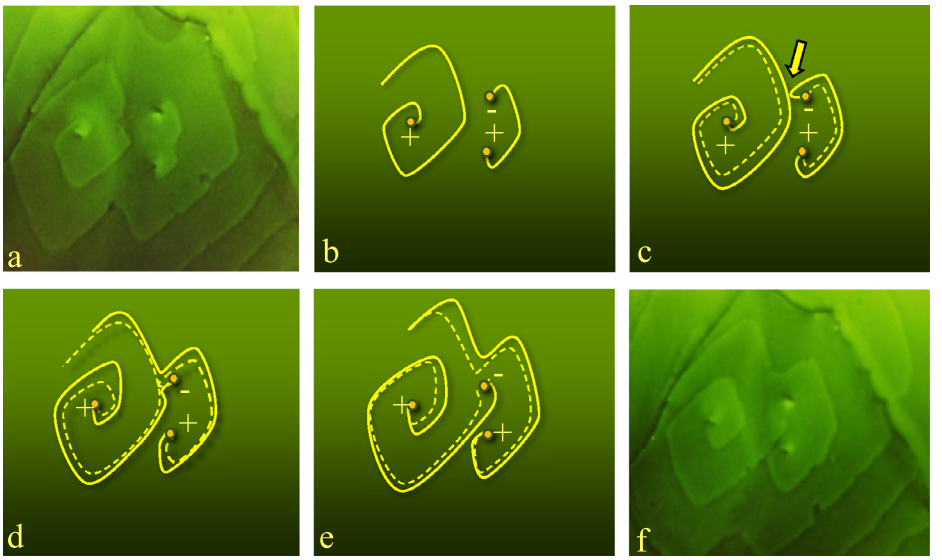

Fig. 13. Observation of growth spirals on the (110) facet of a BPI-in-Isotropic crystal: a and f) photographs of steps taken with a reflecting microscope, b) schematic representation of the initial position of two steps connected to three dislocations labeled as +, + and −, c) the arrow points two steps coming into a contact during their motion (former position of steps is drawn with a dashed line), d) result of the recombination of the two steps, f) further motion of steps resulting from recombination. (Collaboration with P.E. Cladis and R. Barbet-Massin.)

their Burgers vectors must have the $\overrightarrow{b}_{\perp}$ components of opposite signs. If, for example, $\overrightarrow{b}_2 = (111)$, then $\overrightarrow{b}_3$ can be either $(-1\ -1\ 1)$ or $(-1\ -1\ -1)$. From the sense of the spiral shape of the step connected to dislocation 3, we can infer that $\overrightarrow{b}_1$ can be either (111) or $(1\ 1\ -1)$. In summary, we have:

$$\overrightarrow{b}_{\perp 1} = \overrightarrow{b}_{\perp 2} = -\overrightarrow{b}_{\perp 3} \tag{9}$$

For this reason, in Fig. 13, the three dislocations are labeled simply with + and − signs. Here we show the motion of steps during the growth of the BPI crystal from the isotropic phase. In Fig. 13a, dislocations 2 and 3 are connected by one step and another step is connected to the dislocation 1. The motion of steps leads to their "collision" (indicated by the arrow), and after recombination dislocations 1 and 3 are connected by one step and dislocation 2 is connected to another step. In Fig. 13e, a new collision occurs and, after recombination, the initial configuration will be recovered. In conclusion, during crystal growth, dislocation 3 "−" is alternatively connected to the two "+" dislocations, 1 and 2.

3.4. Splitting of steps

A critical reader has certainly detected an unexpected feature in Fig. 11c: not one but two steps are connected to each one of the three dislocations emerging at the BPI/glass interface. One could therefore think that the Burgers vectors of dislocation are (220) and not (111) as we have assumed. In such a case, each dislocation would be a superposition of two elementary dislocations whose Burgers vectors would satisfy the equality $(111) + (1\ 1\ -1) = (220)$. If this explanation was correct, then the two steps in each pair would offer the same optical contrast. Obviously this is not the case: in Fig. 11c one dislocation in each pair is more contrasted than the other one. We will show below that this asymmetric splitting of steps connected to elementary dislocations is due to an important topological detail of the BPI structure.

As it has been said above, BPI can be seen as a periodic network of disclinations. For symmetry reasons, disclinations should coincide with the three-fold axes which in the $I4_132$ symmetry group do not intersect. The whole set of disclinations is thus composed of six subsets which can be labeled as (110), $(1\ -1\ 0)$, (101), $(1\ 0\ -1)$, (011) and $(0\ 1\ -1)$. The (110) subset, pertinent for the present discussion, is represented in Fig. 14b. In this subset, disclinations are organized into alternating sheets S_{-111} and S_{1-11}, in which they are parallel respectively to $[-1\ 1\ 1]$ and $[1\ -1\ 1]$ axes.

In the frame of Wulff's theory of faceting (for recent and pedagogical versions of it, see the books by P. Nozières [23] and by J. Villain and A. Pimpinelli [24]) the occurrence of the (110) facet is related to the existence of a cusp-like minimum in the surface energy γ plotted as a function of the deviation $\vec{\delta m}$ of the surface normal $\vec{m}$ from the [110] axis. The detailed shape (angular discontinuity) of this cusp-like minimum depends on the energy of the steps on the (110) facet, which in turn is related to their height h. In BPI, the height of the steps on the (110) facet corresponds likely to distances between sheets containing disclinations. Such as they are drawn in Fig. 14, the sheets S_{-111} and S_{1-11} seem to be related by some symmetry element. If the Blue Phase I was not chiral, its space group symmetry would be the one of the gyroid surface: *Ia3d*. As we will see in the next section (Fig. 18f or Fig. 19a), the *Ia3d* space group effectively contains a non-symmorphic operation – the *d*-glide plane – which interchanges the sheets S_{-111} and S_{1-11}. However, due to the chirality of the Blue

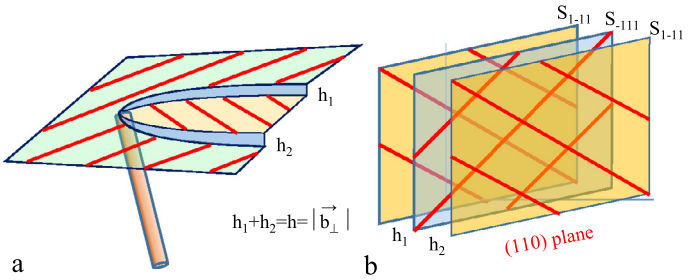

Fig. 14. Splitting of steps: a) a perspective view of a splitted step, b) three successive planes containing disclinations.

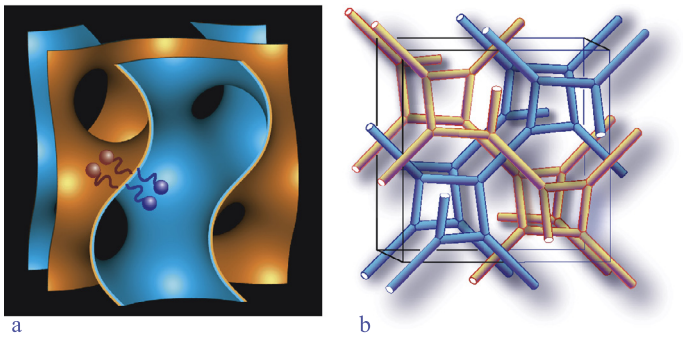

Fig. 15. Structure of the bicontinuous lyotropic phase *Ia*3*d*: a) bilayer made of surfactant molecules oriented with their hydrophobic tails toward the minimal surface called gyroid (G), b) the two labyrinths separated by the bilayer are filled with water. **Remark**: The two sides of the gyroid and the two labyrinths are drawn with different colors for a better visibility but, as the *d*-glide plane symmetry operation of the space group *Ia*3*d* (see Fig. 18b) exchanges the two labyrinths, they should have the same colors.

Phase I, this mirror symmetry is missing, so that the detailed patterns of the S_{-111} and S_{1-11} can be different. This explains why the two steps connected to dislocations in Fig. 11c are not identical. Remark: an elementary screw dislocation emerging on the (100) facet of a silicon crystal would also be connected to two "sub-steps" as those shown in Fig. 1.1 of Ref. [24]. Here the steps have the same height because they are related by a 4_2 screw axis.

4. Lyotropic liquid crystals

4.1. Inverted bicontinuous phases, topological oddities

In inverted bicontinuous lyotropic mesophases, surfactant molecules form bilayers having shapes of minimal surfaces. As an example, we show in Fig. 15 the structure of the *Ia*3*d* phase built around the periodic minimal surface G that we used already in section 3.2 to generate the structure of the Blue Phase I of symmetry $I4_132$ (see Fig. 10). This structural similarity results from geometrical frustrations occurring in both systems. In the case of BPI, we had to cope with the chiral frustration and the occurrence of the periodic network of disclinations is its fingerprint. The geometrical frustration in the *Ia*3*d* phase could be called Gaussian because the local tendency of molecules self-assembled into one bilayer is to generate a negative Gaussian curvature in it. As it is topologically impossible to satisfy this local tendency globally, the bilayer takes the "least bad" shape of the periodic minimal surface *G* surface bearing a system of flat points distributed on three-fold axes.

In general, the inverted bicontinuous lyotropic phases built around minimal surfaces (see Fig. 16) are topological oddities similar to Blue Phases: the *Ia*3*d* phase is thus similar to BPI ($I4_132$), the *Pn*3*m* phase shares the periodic minimal surface D with BPII($P4_232$), the *Im*3*m* phase is analogous to the very first model of a Blue Phase proposed by Alfred Saupe [25] (so far, not observed in experiments). Finally, the so-called sponge phase L_3, organized around a random minimal surface, could be similar to the Blue Fog.

4.2. Nucleation of steps on facets of the Ia3d lyotropic crystals

Observations of steps on facets of the *Ia*3*d* lyotropic crystals was made using the setup depicted in Fig. 17a [28]. The sample – a small droplet of the surfactant (monoolein) – is located on a glass plate in thermal contact with a copper part whose temperature T_s is finely regulated. The sample is surrounded by water vapors whose partial pressure depends on the temperature T_r of a reservoir of water, regulated independently of T_s. When T_r is fixed for example at 30 °C and T_s decreases from 40 °C to 30 °C, then the relative humidity around the sample increases from 55% to 100%, as shown in

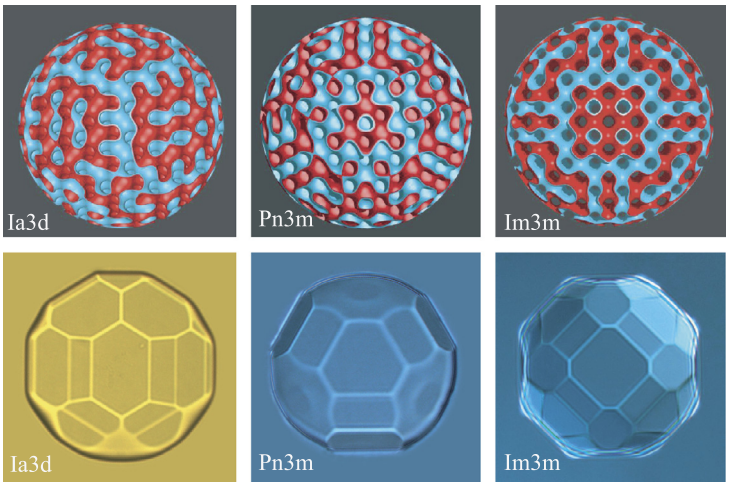

Fig. 16. Inverted bicontinuous lyotropic phases. Upper row: spherical domains cut out from periodic minimal surfaces. Lower row: experimentally observed faceted crystal habits. (Collaboration with W. Gozdz and L. Latypova [26,27].)

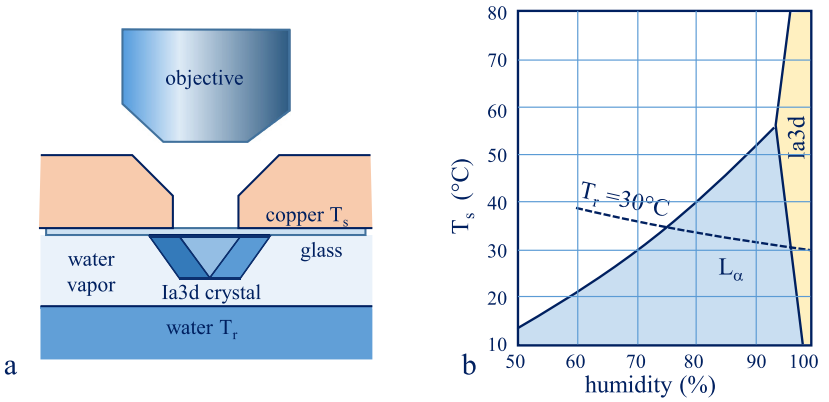

Fig. 17. Observation of steps on facets of the *Ia3d* crystals: a) scheme of the setup, b) phase diagram of the monoolein/water system. (Collaboration with S. Leroy [28].)

Fig. 17b. By this means, the successive phase transitions $L_2 \Rightarrow L_\alpha$ and $L_\alpha \Rightarrow Ia3d$ are driven and well-faceted *Ia3d* crystals can be obtained.

By means of a transmitted light microscope working in phase-contrast mode, the occurrence of steps on (110) and (211) facets has been observed. In Fig. 18a–d, we see the nucleation of successive steps (1, 2, 3 and 4) on the (110) facet. As depicted in Fig. 18e and f, successive steps are related by the *d*-glide plane symmetry = reflection in the mirror plane followed by the partial translation $\vec{d} = (1/2, 1/2, -1/2)$. Being related by this symmetry element, all steps on the (110) facet have the same height and offer the same optical contrast. Let us remind that as already stressed in section 3.3, on the (110) facet of BPI successive steps are differently contrasted because in the $I4_132$ space group the *d*-glide plane is missing.

Not only identical heights of partial steps result from the *d*-glide plane symmetry. Shapes of successive steps are related by the *d*-glide plane symmetry too. Let us stress that in Fig. 18 shapes of partial steps are not rhombic, like the (110) facets, but elongated parallelograms whose two pairs of opposite sides have different mobilities. This anisotropy is allowed by the two-fold symmetry axis orthogonal to the (110) facet.

4.3. Steps connected to dislocations emerging on the (110) facet

Beside the nucleation of steps on the (110) facet discussed above, the growth of *Ia3d* crystals by spiraling motion of steps connected to dislocations was observed too. In Fig. 19b, we see two spiraling steps connected to one dislocation emerging on the (110) facets. The Burgers vector of this dislocation is an elementary one $\vec{b} = (1\ 1\ -1)$ and the two steps connected to it can be said to be "partial" because they result from the splitting $(1\ 1\ -1) = 2\vec{d}$ illustrated in Fig. 19a.

The complex shape of steps observed in experiment (Fig. 19b) is a consequence of the anisotropic mobility discussed previously. In Fig. 19c, fast and slow segments of steps are drawn with respectively red and blue lines. The fast segments catch up the slow ones and one observes the formation of "double" steps depicted in Fig. 19d and observed in the experiment.

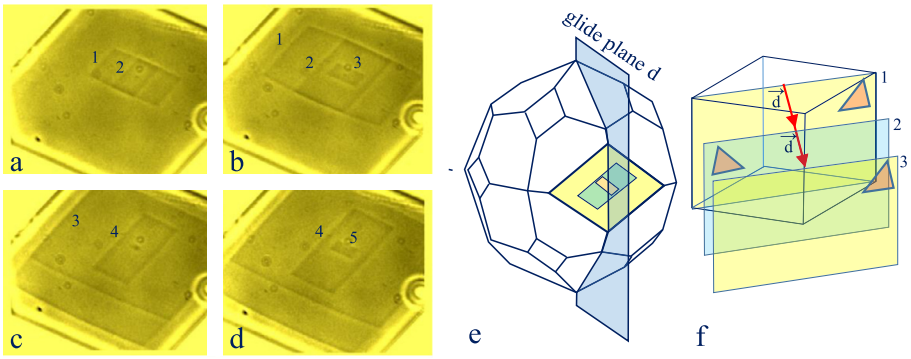

Fig. 18. Steps on the (110) facet of a *Ia*3*d* crystal: a–d) nucleation of successive steps, e) glide plane d, f) successive (110) planes related by the glide plane symmetry. (Collaboration with S. Leroy [28].)

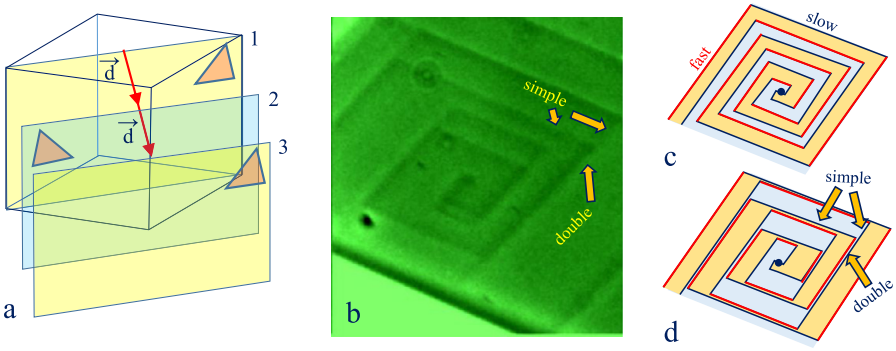

Fig. 19. Splitting of the step connected to the dislocation emerging on the (110) facet of the *Ia*3*d* crystal: a) equivalent (110) planes related by the *d*-glide plane symmetry, b) spiraling steps connected to a dislocation with the Burgers vector $\vec{b} = (1\ 1\ -1) = 2\vec{d}$, c) splitting of the step into two "partial" steps, red and blue sections of the two partial steps are respectively fast and slow, d) result of the anisotropic mobility of partial steps. (Collaboration with S. Leroy [28].)

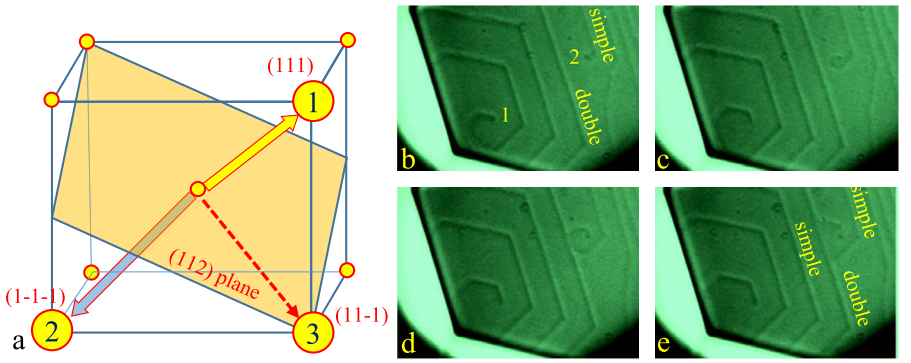

Fig. 20. Three types of dislocations emerging on the (112) facet: a) Burgers vectors **1**(111) and **2**(1-1-1) are oblique with respect to the (112) plane while **3**(11-1) is parallel to it, b-e) motion and recombination of double and simple steps connected to dislocations of types **1** and **2** [28].

4.4. Steps connected to dislocations emerging on the (112) facet

Steps connected to dislocations emerging on (112) facets of *Ia*3*d* lyotropic crystals have been observed too.

Theoretically, dislocations emerging on the (112) facet can be divided in three classes following their Burgers vectors (see Fig. 20a):

1. such as **1**(111), which give rise to double steps
2. such as **2**(1 −1 1), which give rise to simple steps
3. such as **3**(1 1 −1) parallel to the (112) plane, which do not give rise to steps.

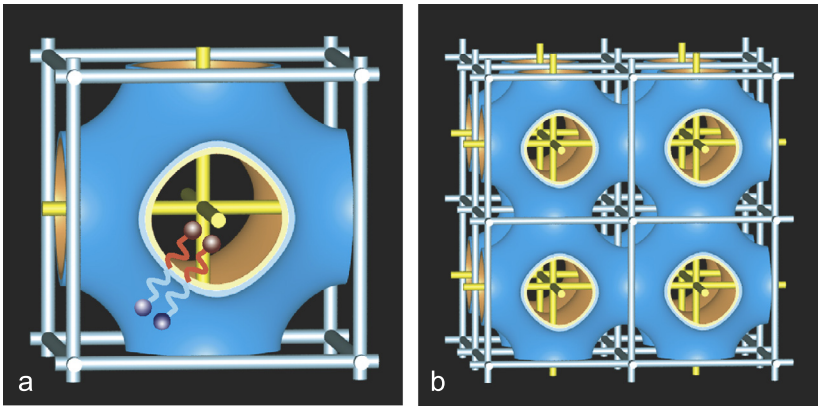

Fig. 21. Structure of the inverted *Im*3*m* lyotropic phase: a) surfactant bilayer inside one cubic unit cell. b) Assembling of he whole crystal from unit cells. One distinguish two labyrinths separated by the bilayer (nodal approximation).

In the series of four images in Fig. 20b–e, we see the motion of double and simple steps connected to dislocations labeled as 1 and 2. Let us suppose that the Burgers vector of the dislocation **1** in Fig. 20b is **1**(111) as indicated in Fig. 20a. The Burgers vector of the dislocation **2** has been indexed as **2**(1 −1 −1) instead of (1 −1 1) because the simple step connected to this dislocation rotates in the sense opposite to the one of the dislocation **1**. The same conclusion is inferred from the observation of the collision of the two steps followed by their recombination.

*4.5. Trivial and Möbius dislocations in Pn*3*m and Im*3*m crystals*

Generation of a dislocation line by the Volterra [29] process is presented by Jacques Friedel in the section 1.2 of his book as a series of four operations:

1. Cut the medium along an arbitrary surface *S*, bounded by line L.
2. Displace the lips *S*1 and *S*2 of the cut relative to each other.
3. Fill with matter the void thus created (or remove any extra matter).
4. Stick the matter along surfaces *S*1 and *S*2, and remove the external forces applied during this operation.

When the translation vector of the second operation $\overrightarrow{b}$ (the Burgers vector) belongs to the Bravais lattice of the crystal, the whole process does not leave in the crystal other "scars" than the core of the disclination line.

In the case of the bicontinuous lyotropic phase *Ia*3*d*, the Volterra process using vectors of the bcc lattice preserves the continuity of the bilayer as well as the continuity of the two labyrinths separated by it.

In the case of *Pn*3*m* and *Im*3*m* (see Fig. 21) lyotropic crystals, generation of dislocations by the Volterra process is more subtle. Let us start the *Pn*3*m* structure. The series of eight images in Fig. 22b–i shows the process of generation of a screw dislocation passing through the South and North poles of a spherical domain on the *Pn*3*m* crystal. The crystal is oriented with its (110) plane parallel to the page surface. The cut surface *S*, represented by the dotted red line in Fig. 22b, is orthogonal to the page surface and is bounded by the NS line. The relative displacement of the lips S1 and S2 is vertical as it can be easily seen in the next pictures.

In Fig. 22f, the displacement is $\overrightarrow{b}_{\mathrm{M}}$, which is the shortest vector of the simple cubic Bravais lattice of the *Pn*3*m* crystal. As expected, after gluing the two lips together we obtain a perfectly continuous and smooth bilayer. However, one detail is disturbing: there is a color discontinuity on the surface at the cut surface.

In his Nobel Prize lecture Lord Rayleigh said: *It is a good rule in experimental work to seek to magnify a discrepancy when it first presents itself, rather than to follow the natural instinct of trying to get quit of it.* In the present case, we could easily get rid of this color discontinuity by drawing the two sides of the bilayer with the same color as we should do in order to respect the *Pn*3*m* symmetry. However, by using two colors instead of one, we have discovered something new: the Volterra process with displacement $\overrightarrow{b}_{\mathrm{M}}$ makes the bilayer unorientable like the Möbius strip. In other words, the Volterra process with displacement $\overrightarrow{b}_{\mathrm{M}}$ produces a "Möbius" dislocation.

When the displacement of the lips is continued, as shown if Fig. 22g–i, we obtain a dislocation with the Burgers vector $\overrightarrow{b}_{\mathrm{T}} = 2\overrightarrow{b}_{\mathrm{M}}$ and the bilayer recovers its orientability. If, instead of vector $\overrightarrow{b}_{\mathrm{T}}$, we used the vector $\overrightarrow{b'}_{\mathrm{T}}$ defined in Fig. 22a, we would also obtain a dislocation preserving the orientability of the bilayer. In both cases, the dislocation is "trivial", in contradistinction with Möbius dislocations.

Dislocations in an *Im*3*m* crystal can also be of Möbius and trivial types (see Fig. 23). When the Burgers vector $\overrightarrow{b}_{\mathrm{T}}$ (defined in Fig. 23a) of the dislocation belongs to this sc lattice, the continuity of the bilayer as well of that of the two labyrinths separated by it is preserved. This is obvious in Fig. 23d. However, when Burgers vector $\overrightarrow{b}_{\mathrm{M}}$ (defined in Fig. 23a)

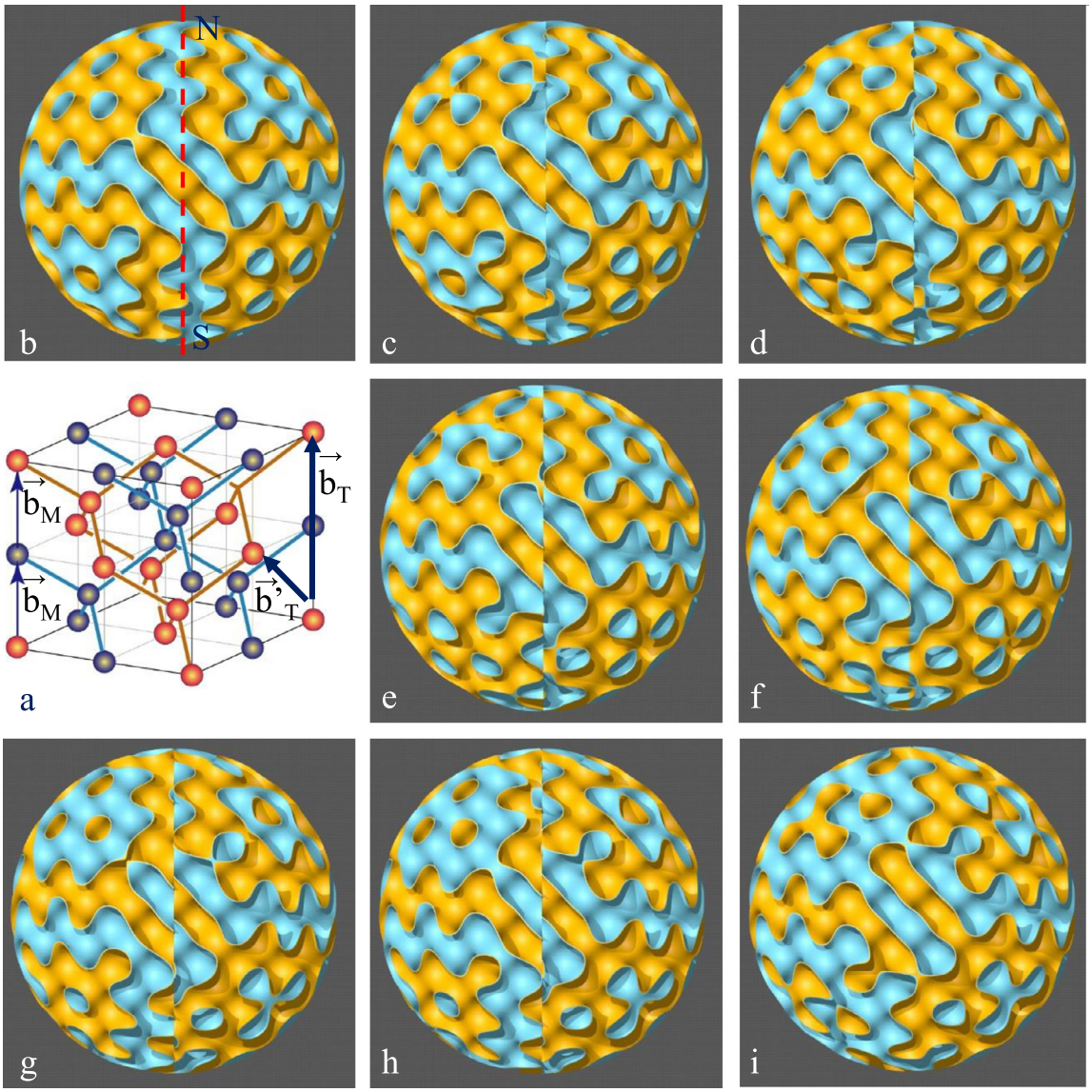

Fig. 22. Trivial and Möbius dislocations in *Pm*3*n* crystals: a) definitions of Burgers vectors, b) spherical domain of the perfect *Im*3*m* crystal (the dotted red line indicates the cut surface orthogonal to the page surface), c–f) generation of a "Möbius" dislocation by the Volterra process using vector $\mathbf{b}_M$, c–i) generation of a "trivial" dislocation by the Voterra process using vector $\mathbf{b}_T$.

is used in the Volterra process, the bicontinuous topology of the *Im*3*m* structure is affected: the bilayer loses its orientability as shown in Fig. 23c.

So far dislocations emerging on the (111) facet of a *Pn*3*m* crystal and connected to steps have been observed in the monoolein/water binary system. Are they of "trivial" or Möbius type? From the chapter 2 "Elastic theory of dislocations" of Jacques Friedel's book, we know that there are two contributions to the energy per unit length of dislocations:

$$W = \frac{\mu b^2}{4\pi K} ln \frac{r_1}{r_o} + W_c \tag{10}$$

The first term accounts for the elastic energy of the deformed crystal considered as an isotropic medium with the shear modulus μ and the Poisson modulus K. The second term represents the energy of the dislocation core of radius r_o. As $\vec{b}_T = 2\vec{b}_M$, the Möbius dislocation is favored by the elastic term.

On the other hand, the core energy of the Möbius dislocation seems to be larger than that of the trivial dislocation, for the following reason. The loss of the orientability of the bilayer is accompanied by the loss of its continuity in the dislocation core: there is a free edge of the bilayer inside the crystal in the dislocation core. As shown in Fig. 24, this free edge forms a closed loop. It emerges from the crystal at the North pole (N, Fig. 24a) follows a very complicated trajectory

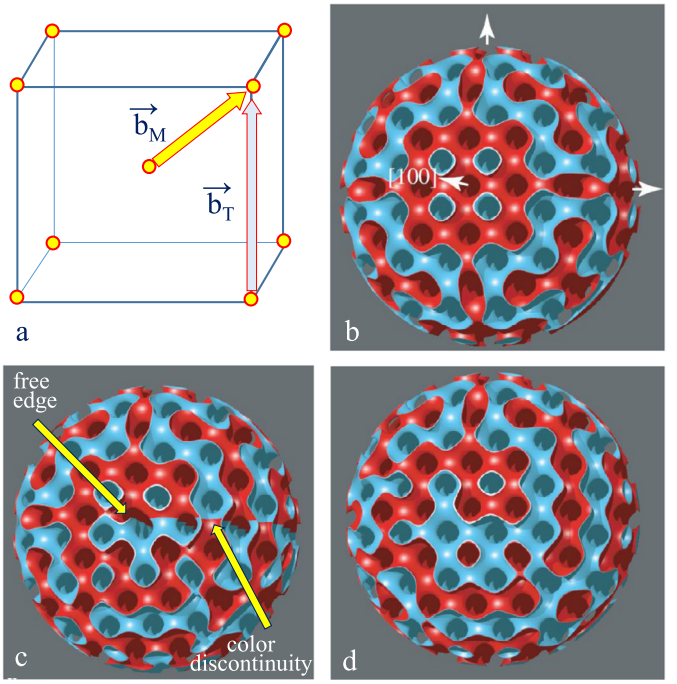

Fig. 23. Trivial and Möbius dislocations in *Im*3*m* crystals: a) definitions of the shortest Burgers vectors belonging to the simple cubic ($\mathbf{b}_T$) and to the bcc ($\mathbf{b}_M$) Bravais lattices, b) spherical domain of the perfect *Im*3*m* crystal, c) the "Möbius" dislocation generated by the Voterra process using vector $\mathbf{b}_M$, d) the "trivial" dislocation generated by the Voterra process using vector $\mathbf{b}_T$.

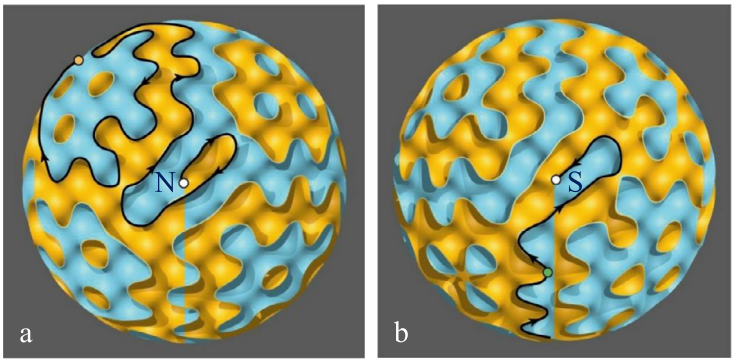

Fig. 24. Free edge of the bilayer forming a closed loop associated with the Möbius dislocation. It follows a complicated trajectory from N to S on the crystal surface and pierces the crystal from S to N.

on the crystal surface arriving at the South pole (S Fig. 24b), where it enters the crystal and returns at the starting point S. Let us emphasize that such free edge in the core of a Möbius dislocation created in the *Im*3*m* crystal is well visible in Fig. 23c. The energy per unit line of the free edge in Möbius dislocations increases the core energy.

4.6. Disorientations in the sponge phase

In the $C_{12}EO_2$/water binary mixture, the *Pn*3*m* phase is known to melt into the sponge phase L_3 [30]. Let us suppose that before the $Pn3m \Rightarrow L_3$ transition, the *Pn*3*m* phase contains a Möbius dislocation. What happens to the Möbius dislocation upon melting? During the $Pn3m \Rightarrow L_3$ transition, only the crystalline position order is destroyed, but the topology of the bilayer is conserved, as it shown on the example of the *Im*3*m* crystal in Fig. 25. We can expect therefore that the free edge accompanying the Möbius dislocation will be conserved. If this is the case, we have to deal with a new kind of topological defect that we propose to call *disorientation* as it alters the orientability of the bilayer.

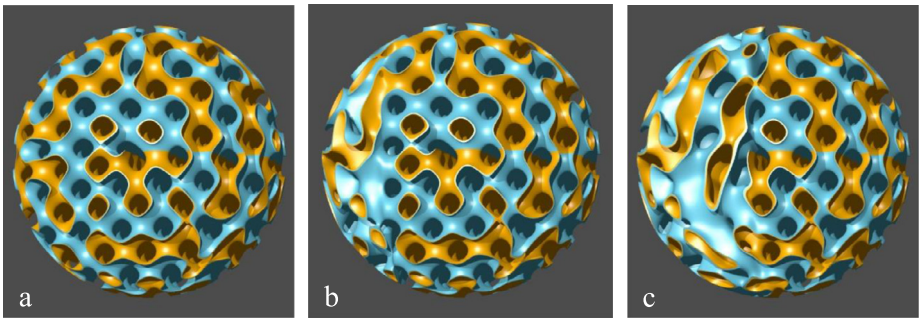

Fig. 25. Melting of the *Im*3*m* crystal containing a Möbius dislocations into the sponge phase.

5. Topological defects

5.1. Analogy between dislocations and vortices in superconductors, TGB phases

In the last section 17.8.3b of his book, Jacques Friedel makes a first step toward the generalization of the concept of dislocation and namely outlines the analogy between dislocations in crystals and vortex lines in superconductors:

"A general theory of these lines can be set up, very similar to that of dislocation lines. The Maxwell equations take place of equations of elasticity; the quantum magnetic flux plays the role of a Burgers vector; magnetic energy is stored within a distance λ *in the superconductive phase around the line, in much the same way as the elastic energy around a dislocation line; formulae for the line tension are similar and come from this long range magnetic energy, more than from core energy in the normal phase; the long range interaction between lines are rather similar to those between dislocations, and the Lorentz force due to transports currents transverse to the magnetic field acts as an external driving force similar to the applied stress."*

Eight years later, P.-G. de Gennes, attracted meanwhile by Jacques Friedel to the Solid State Physics lab in Orsay, extended this analogy in his celebrated paper *An analogy between superconductors and smectics A* [31], where he conjectured on the existence of a system of screw dislocations induced by chirality in smectics A similar to the systems of vortices induced by the magnetic field in superconductors of the second type. It took the next 17 years before the Bell Labs team [32] proved experimentally that this conjecture was true. Today the chiral smectic phase pierced by the system of screw dislocations is known as the Twist Grain Boundary (TGB) phase, because it is made of a system of screw dislocation walls as predicted theoretically by Renn and Lubensky (see, *e.g.*, in [33]).

5.2. Dissociation of dislocation pairs, the hexatic phase

A similar scientific adventure in which dislocations played the main role can be told about the conjecture formulated in 1973 by Kosterlitz and Thouless [34] about the melting of two-dimensional crystals which should occur in two stages: 2D crystal $\Rightarrow$ hexatic phase $\Rightarrow$ isotropic liquid. The intermediate hexatic phase is the result of the dissociation of dislocation pairs preexisting in the 2D triangular crystal. Indeed, as discovered by Kosterlitz and Thouless, the dissociation of dislocations destroys only the positional order but not the orientational one. After the 2D crystal $\Rightarrow$ hexatic phase transition, the directions of bonds between adjacent molecules (atoms or particles) remain correlated.

The resulting orientational order has the sixfold symmetry of the initial 2D crystal lattice and mathematically can be represented as

$$\Psi_6 = |\Psi_6| e^{i\varphi_6(r)} \tag{11}$$

Fourteen years later, Dierker, Pindak, and Meyer [35] discovered that one of smectic phases – SmI – possesses the hexatic orientational order. This beautiful discovery deserves to be mentioned here because the existence of the hexatic order parameter was inferred from the presence of a new type of topological defects: $2\pi/6$ disclinations. As shown in Fig. 26, a $-2\pi/6$ disclination of the hexatic order parameter is similar to the "rotation dislocation in a crystal" represented in Fig. 1.4 of Jacques Friedel's book (see Fig. 27).

5.3. Defects in systems with broken symmetries

Dislocations, disclinations, disorientations or vortices are a few examples of topological defects in systems with broken symmetries. As there is no place here to quote other examples, the best we can do is to recommend several references. As far as dislocations and disclinations are concerned, the very large article *Disclinations, dislocations, and continuous defects: A reappraisal*, written recently by Maurice Kleman and Jacques Friedel [36] describes the state of art in this domain. In the domain of liquid crystals, *The Physics of Liquid Crystals* by P.-G. de Gennes and J. Prost [37] has to be quoted, without forgetting the two volumes written by Patrick Oswald and the author [38,39]. A more general view on defects in condensed

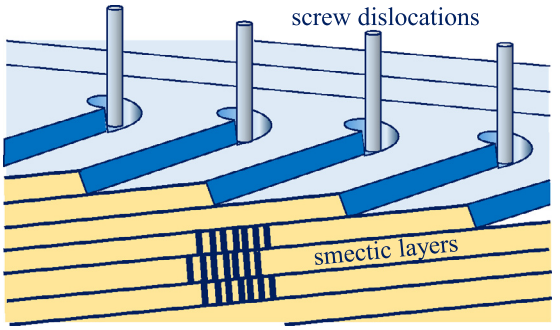

Fig. 26. Twist Grain Boundary made of screw dislocations in the TGB_A smectic phase.

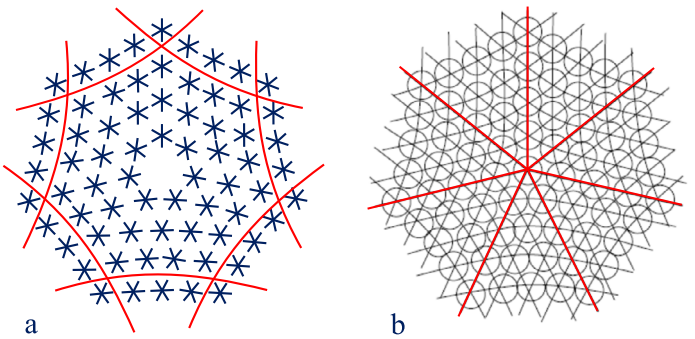

Fig. 27. a) $-2\pi/6$ disclination in the hexatic phase, b) $-2\pi/6$ disclination (rotation dislocation) in the triangular crystal.

matter can be found in books of Chaikin and Lubensky [40] and of Kleman and Lavrentovich [41]. Finally, the world of frustrated systems is treated in the book of Sadoc and Mosseri [42].

6. Out of the rut

6.1. Conformal crystals

When a rotational dislocation is introduced in a 2D crystal by the Volterra process, in its last stage 4 the external forces applied during this operation have to be removed. The crystal reaches then its new, elastically deformed, equilibrium state whose energy is larger than the one of the ground state.

There is however a system, called *conformal crystal*, whose ground states are topologically equivalent to rotational dislocations (or disclinations), namely the 2D system of particles interacting through a power low potential with exponent k and rotating as a whole so that particles are submitted also to the centrifugal force. It has been pointed out by François Rothen and Piotr Pieranski [43] that in the ground state, the particle are disposed on a lattice which is the obtained from the triangular lattice by the conformal transformation

$$w = az^{k/(k+2)} \tag{12}$$

with $z = u + \mathrm{i}v$ and $w = x + \mathrm{i}y$ where (u, v) are the coordinates of points on the triangular lattice, while (x, v) are the coordinates of points on the conformal lattice. As an example, we show in Fig. 28a the ground state obtained with $k = 2$. From a topological point of view, it corresponds to a -2π disclination. Conformal crystals have been observed first in experiments with steel spheres submitted to a magnetic field (see references in [43]). More recently, Drenckhan, Weaire and Cox [44] pointed out that a monolayer of soap bubbles confined between a plane and a sphere adopts the structure of the conformal crystal given by equation (12).

6.2. Locally favored structures

In section 2.4 we have seen that to divide a triangular monolayer into two layers by “up” and “down” motions of nearest neighbors (see Fig. 8a) is an impossible task similar to the one encountered in the Ising antiferromagnetic model on a triangular lattice. In other words, it is impossible to satisfy globally the local tendency of nearest neighbors to form “up” and “down” pairs.

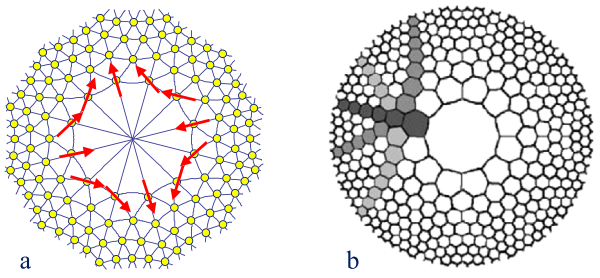

Fig. 28. Conformal crystal generated by equation (12): a) on a rotating disc [43], the system of arrows in proves that topologically it is equivalent to a -2π disclination, b) soap bubbles confined between a sphere and a plan [44].

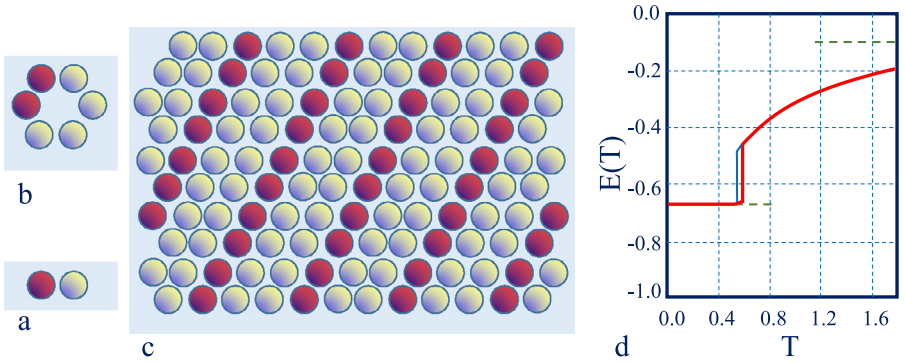

Fig. 29. Locally Favored Structures [45]: a) in the antiferromagnetic Ising model, b) so-called (24) structure, c) one of ground states of the (24) LFS, d) crystal–liquid transition obtained by the Monte Carlo method.

Recently, Ronceray and Harrowell tackled with a more general problem, in which instead of pairwise interactions (Fig. 29a) they considered the so-called Locally Favored Structures (LFS) such a the one in Fig. 29b. This LFS is impossible to satisfy globally so that the ground "crystalline" state (see Fig. 29c) is degenerate and its energy, $-2/3$, is higher than the one of the LFS (-1). The Monte Carlo simulation showed that upon heating, the first-order transition into the "liquid" state occurs (see Fig. 29d).

7. Acknowledgments

It was a great honor for me to be selected by Hélène Bouchiat as one of the contributors to the special issue of CRAS in memory of Monsieur Jacques Friedel, but I was not alone to do the work presented here. Several names have been already quoted in the text, but so many others among my friends, colleagues, coworkers or students would like also to be associated with this tribute in honor of Monsieur Friedel. The "Acknowledgements" section is a perfect place to do this. As the work on topological defects in colloidal crystals and liquid crystals is presented in this paper in chronological order, it seems natural to follow the same order here.

7.1. Le pied à l'étrier

The very first person that I have met in September 1970 in the Solid State Physics Laboratory in Orsay was Monsieur Friedel himself. The interview with him was very short, but in virtue of the butterfly effect it changed the course of my life. The next person, met a moment later, was Michel Héritier, who had to test (successfully, by chance) the level of my education at the Adam Mickiewicz University in Poznań. Finally, a day or two later, I met Étienne Guyon, to whom Monsieur Friedel recommended me as a student. He asked me to start to work immediately (!). Since then, Etienne Guyon directed my work during many years and helped me in all aspects of life. I am deeply indebted to him for his generosity.

Like so many other students of the Friedel's DEA "Physique des solides", I had the chance to listen to his lectures as well as to those of Monsieur André Guinier, whose academic French was easy to understand, in contrast with that of P.-G. de Gennes, extremely picturesque. Being student I worked at the same time with Étienne Guyon on the Rayleigh–Benard convection in nematics. Our experimental setups, tailored for this purpose, were made from quite complex metal parts machined with mastery by Gaston Brisnot and Robert Philippe.

7.2. Colloidal crystals

When working on liquid crystals, I heard from Bob Meyer on a post-doc visit in LPS that suspensions of colloidal particles in deionized water can form crystal structure providing Bragg reflections of visible light. Then during the International Conference on Liquid Crystals in Bordeaux (organized in 1978 by Henry Gasparou and Jacques Prost) one of Japanese participants – S. Mitaku – brought a test tube containing such a colloidal crystal and allowed other participants to play with it. We were all fascinated to see crystals melting upon a gentle shaking!!! Once back home I asked Leszek Strzelecki, a chemist working with Lionel Liebert on liquid crystals, to synthesize polystyrene spheres by the method indicated by Mitaku. Thanks to Leszek, a lot of experiments were made. In particular, the study of structures in confined colloidal crystals was made with mastery by Brigitte Pansu (PhD work). The interest in colloidal crystals was rapidly growing all around the world. François Rothen from Lausanne and Paul Chaikin from Santa Barbara came into the subject of colloidal crystals by what… *I may call geographical accidents*, namely because during their sabbatical stays in LPS François Rothen shared my office, while that of Paul Chaikin was close to mine. A few years later, in 1984, we organized together in Les Houches a winter workshop on colloidal crystals.

7.3. Blue Phases

Having worked on colloidal crystals we built setups well adapted to studies of Blue Phases, liquid crystals brought to our lab by Patricia Cladis from Bell Laboratories. The very first experiments performed with Pat's samples uncovered the beauty of Blue Phases: not only they were providing Bragg reflections like colloidal crystals, but they were also faceted! The beginning of our work on Blue Phases coincided with the arrival of Rémi Barbet-Massin (PhD student). His skills were extremely useful, among other, for the theoretical interpretation of Bragg reflections. We benefited also a lot from our collaboration with Richard Hornreich, whom we have met for the first time during the workshop in Les Houches.

One of the most fascinating properties of Blue Phases is their faceting. When trying to understand its origin we discovered *Leçons de cristallographie* of George Friedel containing the discussion of this problem illustrated by wonderful drawings of crystals habits. By chance, there was a renewal of interest in the faceting. In LPS, we benefited from discussions with Heinz Schulz and from lectures on faceting given in Collège de France by Philippe Nozières.

7.4. Lyotropic liquid crystals

We came to studies of dislocations of lyotropic liquid crystals by what *I may call a happy laboratory accident*. After a long period of experiments with free-standing films of thermotropic smectic phases, we decided to try our luck with lyotropic films. Marianne Impéror-Clerc provided us with a sample of an anionic surfactant $C_{12}EO_6$ that, mixed with water in adequate proportions, gives the lamellar phase suitable for drawing free-standing films. The first experiments were done with an Erasmus student – Daniel Rohe – on practice in my lab. When playing with films in lamellar phase, we were surprised to see that a droplet of the surfactant fallen by accident on a glass window was faceted. We knew from the paper of Jean Charvolin *Crystals of interfaces: the cubic phases of amphiphile/water systems* [46] that cubic phases can be faceted. Faceted shapes of air bubbles in lyotropic cubic phases have also been reported by Paul Sotta [47]. Nevertheless, the faceting we observed was much richer than those reported in [46] and [47]. During his lectures, Philippe Nozières explained to us that at 0 K the so-called devil staircase faceting can occur, but our experiments were made at room temperature! It was therefore obvious that faceting of lyotropic liquid crystals is a challenging subject.

The outburst of this new subject coincided with the invitation of Bertrand Deloche to give "in tandem" with him lectures on soft matter: polymers and liquid crystals. Previously, during many years I had been giving lectures on thermotropic liquid crystals; the book written with Patrick Oswald is a summary of our lectures [38,39]. Stimulated by Bertrand Deloche, I decided to give lectures on lyotropic liquid crystals, which I knew only a little. Preparation of these new lectures consisted in doing new experiments. Most of them were done with students on practice in our lab and with a PhD student of W. Gozdz, Larisa Latypova. Among these experiments, the detection of steps on surfaces of cubic crystals and of dislocations connected to steps was the most challenging. Samuel Leroy, a student from the "École normale" in Lyons, came to Orsay for a summer practice and accepted this challenge with success.

8. Epilog, a travel in time

The last Fig. 30 of my contribution shows 25 umbilics, topological defects, generated in a nematic layer by magnetic and electric fields in a way that their pattern is the one of a clock. The purpose of this image is not to show topological defects again, but to call on mind the passing time. In this paper, we traveled in time more than half a century ago, because the French edition of *Dislocations* was published in 1956 when Monsieur Friedel was already 35.

In the first chapter, "Les signes du passé" of his autobiography *Graine de mandarin*, Monsieur Friedel travels in time to the sources of his life and remembers the happy days of his youth passed in "Graf", the family house situated close to the Ill River. I read these admirable pages in 1994, having bought this book immediately after its publication. A few days later, I met Monsieur Friedel and asked him a few questions about some facts concerning Georges Friedel and Marie Curie reported in his book.

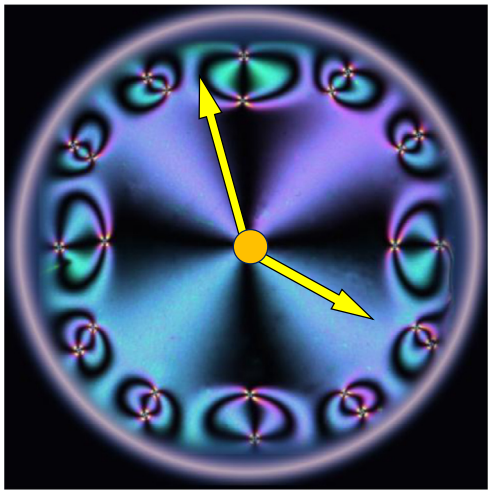

Fig. 30. A system of 25 umbilics generated by magnetic and electric fields in a nematic layer.

"Mon cher Pieranski, he said, you should not have to buy my book because one copy of it is waiting for you in the office of Madame Coule (the secretary of M. Friedel)."

The book was there in a big stack of other copies waiting for other members of our lab. Once back in my office, I opened it and on the front page I discovered a handwritten dedication:

"*Mon cher Pieranski, ceci vous donnera une image complémentaire de G. Friedel. Amicalement, J. Friedel*"

References

[1] J. Friedel, Graine de mandarin, Éditions Odile Jacob, Paris, 1994.
[2] W.K. Burton, N. Cabrera, F.C. Frank, The growth of crystals and the equilibrium structure of their surfaces, Philos. Trans. R. Soc. Lond. Ser. A, Math. Phys. Sci. 243 (1951) 299–358.
[3] F.C. Frank, Crystal growth award of the American association for crystal growth, J. Cryst. Growth 46 (1979) 591–594.
[4] One of referees remarked that this quotation of F.C. Frank could misleadingly be taken as an universal rule. Actually, not all crystals are full of dislocations like metals submitted to metalworking processes. On the contrary, huge, 30 cm in diameter, silicon crystals grown by the Czochralski method and used for production of wafers in electronic industry are dislocation-free!.
[5] Jacques Friedel, Dislocations, Pergamon Press, 1964.
[6] D.W. Schaefer, B.J. Ackerson, Melting of colloidal crystals, Phys. Rev. Lett. 35 (1975) 1448–1451.
[7] N.A. Clark, A.J. Hurd, B.J. Ackerson, Single colloidal crystals, Nature 281 (1979) 57–60.
[8] P. Pieranski, Colloidal crystals, Contemp. Phys. 24 (1983) 25–73.
[9] F. Rothen, in: Proceedings of Winter Workshop on Colloidal Crystals, J. Phys. (Paris) 46 (1984), Colloque C3.
[10] P. Pieranski, Microspectroscopy, in: Proceedings of Winter Workshop on Colloidal Crystals, J. Phys. (Paris) 46 (1984), C3-281–293, Colloque C3.
[11] P. Pieranski, L. Strzelecki, J. Friedel, Observation of edge dislocations in ordered polystyrene latexes, J. Phys. (Paris) 40 (1979) 853–859.
[12] B. Pansu, P. Pieranski, L. Strzelecki, Thin colloidal crystals: a series of structural transitions, J. Physique 44 (1983) 531–536.
[13] P. Pieranski, L. Strzelecki, B. Pansu, Thin colloidal crystals, Phys. Rev. Lett. 50 (1983) 500–503.
[14] D.H. Van Winkle, C.A. Murray, Layering transitions in colloidal crystals as observed by diffraction and direct-lattice imaging, Phys. Rev. A 34 (1986) 562–573.
[15] B. Pansu, P. Pieranski, P. Pieranski, Structures of thin layers of hard spheres: high pressure limit, J. Phys. (Paris) 45 (1984) 331–339.
[16] M. Schmidt, H. Löwen, Phase diagram of hard spheres confined between two parallel planes, Phys. Rev. E 55 (1997) 7228–7241.
[17] Y. Shokef, Y. Han, A. Souslov, A.G. Yodhd, T.C. Lubensky, Buckled colloidal monolayers connect geometric frustration in soft and hard matter, Soft Matter 9 (2013) 6565–6570.
[18] The Friedel–Donnay–Harker rule: "the prominence order of the facets of a crystal is the same as the decreasing order of the interplanar distances, taking into account an eventual reduction by a factor of two, three or four as a result of the group space symmetries". In the case of the space group $I4_132$, the fourfold screw axis 4_1 perpendicular to the (100) facet reduces the interplanar distance by the factor of four. As a result the height of elementary steps, on the (100) facet is reduced by the factor of four. Such small terraces are easier to nucleate and the (100) facet becomes very instable.
[19] F.C. Phillips, An Introduction to Crystallography, Longmans, New York, 1960.
[20] Georges Friedel, Leçons de cristallographie, Librairie Scientifique Albert Blanchard, Paris, 1964.
[21] Hui-Chuan Cheng, Jin Yan, Takahiro Ishinabe, Norio Sugiura, Chu-Yu Liu, Tai-Hsiang Huang, Cheng-Yeh Tsai, Ching-Huan Lin, Shin-Tson Wu, J. Disp. Technol. 8 (2012) 98–103.
[22] P.P. Crooker, Blue phases, in: H.-S. Kitzerow, C. Bahr (Eds.), Chirality in Liquid Crystals, Springer, 2001, Chapter 7.
[23] P. Nozières, Shape and growth of crystals, in: C. Godreche (Ed.), Solids Far from Equilibrium, Cambridge University Press, 1992, Chapter 1.
[24] J. Villain, A. Pimpinelli, Physique de la croissance crustalline, Aléa Saclay, Eyroles, 1995. English version: J. Villain, A. Pimpinelli, Physics of Crystal Growth, Cambridge University Press, 1998.
[25] A. Saupe, On molecular structure and physical properties of thermotropic liquid crystals, Mol. Cryst. Liq. Cryst. 7 (1969) 69–74.
[26] L. Latypova, W. Gozdz, P. Pieranski, Symmetry, topology and faceting in bicontinuous lyotropic crystals, EPJE 36 (2013) 88.
[27] L. Latypova, W. Gozdz, P. Pieranski, Facets of lyotropic liquid crystals, Langmuir 30 (2014) 488–495.

[28] S. Leroy, P. Pieranski, Steps and dislocations in cubic lyotropic crystals, J. Phys. Condens. Matter 18 (2006) 6453–6468.
[29] V. Volterra, Équilibre des corps multiplement connexes, Ann. Sci. Éc. Norm. Super. 24 (1907) 401. It is interesting to emphasize that the concept of dislocations as well as their existence in crystals was unknown to Vito Volterra who was only interested in solutions of equations of elasticity in multiply connected continuous elastic media such as a hollow cylinder. Nevertheless, the Volterra work was certainly seminal because it opened new perspectives and inspired other great minds.
[30] M.L. Lynch, K.A. Kochvar, J.L. Burns, R.G. Laughlin, Aqueous-phase behavior and cubic phase-containing emulsions in the $C_{12}E_2$-water system, Langmuir 16 (2000) 3537–3542.
[31] P.-G. de Gennes, An analogy between superconductors and smectics A, Solid State Commun. 10 (1972) 753–756.
[32] J.W. Goodby, M.A. Waugh, S.M. Stein, E. Chin, R. Pindak, J.S. Patel, Characterisation of a new helical smectic liquid crystal, Nature 337 (1989) 449–452.
[33] T.C. Lubensky, On "An analogy between superconductors and smectics A", in: P.G. de Gennes Impact on Science, vol. 1, World Scientific, 2009.
[34] J.M. Kosterlitz, D.J. Thouless, Ordering, metastability and phase transitions in two-dimensional systems, J. Phys. C 6 (1973) 1181–1203.
[35] S.B. Dierker, R. Pindak, R.B. Meyer, Consequences of bond-orientational order on the macroscopic orientation patterns of thin tilted hexatic liquid-crystal films, Phys. Rev. Lett. 68 (1986) 1819–1822.
[36] M. Kleman, J. Friedel, Disclinations, dislocations, and continuous defetcs: a reappraisal, Rev. Mod. Phys. 80 (2008) 61–80.
[37] P.-G. de Gennes, J. Prost, The Physics of Liquid Crystals, Oxford University Press, 1993.
[38] P. Oswald, P. Pieranski, Nematic and Cholesteric Liquid Crystals, Taylor & Francis, 2005.
[39] P. Oswald, P. Pieranski, Smectic and Columnar Liquid Crystals, Taylor & Francis, 2006.
[40] P.M. Chaikin, T.C. Lubensky, Principles of Condensed Matter Physics, Cambridge University Press, 1995.
[41] M. Kleman, O.D. Lavrentovich, Soft Matter Physics: An Introduction, Springer, 2003.
[42] J.-F. Sadoc, R. Mosseri, Geometrical Frustration, Cambridge University Press, 1999.
[43] F. Rothen, Piotr Pieranski, Mechanical equilibrium of conformal crystals, Phys. Rev. E 53 (1996) 2828–2842.
[44] W. Drenckhan, D. Weaire, S.J. Cox, The demonstration of conformal maps with two-dimensional foams, Eur. J. Phys. 25 (2004) 429–438.
[45] P. Ronceray, P. Harrowell, The variety of ordering transitions in liquids characterized by a locally favoured structure, Europhys. Lett. 96 (2011) 36005.
[46] J. Charvolin, Crystals of interfaces: the cubic phases of amphiphile/water systems, in: Proceedings of Winter Workshop on Colloidal Crystals, J. Phys. (Paris) 46 (3) (1984), Colloque C3.
[47] P. Sotta, Equilibrium shape of lyotropic cubic monocrystals, J. Phys. (Paris) II 1 (1991) 763–772.